Intracerebral hemorrhage alters α2δ1 and thrombospondin expression in rats

BINGQIAN WANG[1,2], XIAOPENG LI[1,3], NING YU[1], LIANG YANG[1], CHENGRUI NAN[1], LISI GUO[1] and ZONGMAO ZHAO[1]

[1]Department of Neurosurgery, The Second Hospital of Hebei Medical University, Shijiazhuang, Hebei 050000; [2]Department of Neurosurgery, Affiliated Xing Tai People Hospital of Hebei Medical University, Xingtai, Hebei 054000; [3]Department of Neurosurgery, The First Hospital of Handan City, Handan, Hebei 056000, P.R. China

Received October 12, 2021; Accepted January 19, 2022

DOI: 10.3892/etm.2022.11256

Abstract. Calcium voltage-gated channel auxiliary subunit (α2δ1) is a non-essential subunit of the voltage-gated calcium channel complex and is ubiquitously expressed in a number of tissues, including the brain. Thrombospondin (TSP)1 and TSP2 are extracellular matrix proteins and belong to the multi-domain glycoprotein family of macromolecular oligomers. TSP1/2 and α2δ1 promote synapse formation and functional recovery following cerebral infarction. However, to the best of our knowledge, the expression levels of α2δ1 and TSP1/2 in brain tissues, and the effects of intracerebral hemorrhage (ICH) on these levels have not yet been elucidated. The present study established a rat model of hemorrhage induced by injecting collagenase IV into the striatum to determine the changes in α2δ1 and TSP1/2 expression following ICH. The protein expression levels of α2δ1 and TSP1 in the striatum after hemorrhage were significantly increased on day 5 and returned to baseline levels on day 21; however, the protein expression levels of TSP2 were decreased on day 5, whereas they increased on day 14, subsequently returning to baseline levels. In addition, using proteomics analysis of tissues from the sham group (saline injection) and at 24 h post-ICH, it was found that both α2δ1 and TSP1 interacted with neural EGFL like 2. Taken together, these findings suggested that the expression levels of α2δ1 and TSP1/2 were altered in brain tissues in response to ICH.

Introduction

Patients with intracerebral hemorrhage (ICH) have high disability and mortality rates, and the survivors suffer from a variety of neurological dysfunctions (1). The death of neurons during cerebral hemorrhage may lead to a decrease in the number of synapses (2). It has been demonstrated that the number of synapses increases gradually during the recovery period following cerebral infarction (3,4). Although extensive studies on the mechanisms of ICH have been performed, the underlying mechanisms remain largely unknown (5,6).

It has been demonstrated that thrombospondin ½ (TSP1/2) and its receptor, calcium voltage-gated channel auxiliary subunit (Cacna2δ1; α2δ1), promote the formation of synapses and synaptogenesis (7). α2δ1 was originally isolated from skeletal muscle as a non-essential subunit of the L-type voltage-gated calcium channel complex (8). It is widely expressed in a number of tissues, including neurons (9,10). α2δ1 expression is altered in several pathophysiological conditions. In this regard, neuropathic pain is associated with increased α2δ1 expression in the dorsal root ganglion and spinal cord (11). Furthermore, α2δ1 expression is increased in cerebral ischemia-reperfusion injury (12). A recent study has also indicated that ICH increases the expression levels of α2δ1 and glutamate NMDA receptor subunit ζ1 (13). TSPs are multi-domain calcium-binding extracellular glycoproteins mediating cell-cell and cell matrix interactions (14,15). TSPs can be categorized into two subfamilies: Trimer subgroup A (TSP1 and TSP2) and pentamer subgroup B (TSP3, TSP4 and TSP5) (16-18). Each of these five TSPs is encoded by a separate gene. It has been reported that TSP1 and TSP2 exhibit increased expression levels in brain tissues affected by hemorrhage, to regulate angiogenesis through their anti-angiogenic properties (19). TSP1/2 binding to α2δ1 serves a crucial role in promoting synaptic formation and synaptogenesis (20,21). TSP1 also enhances the migration and adhesion of macrophages, smooth muscle cells (SMCs) and fibroblasts into the vessel walls, and promotes the migration and proliferation of SMCs (22). TSP1 is highly expressed in the ischemic brain (4,23). Therefore, it was hypothesized that alterations in the levels of TSP1/2 and α2δ1 affect synaptogenesis during hemorrhagic injury. In the present study, the expression levels of TSP1/2 and α2δ1 were measured in a rat model of ICH established by injecting collagenase IV into the rat striatum. The present study aimed to provide insights that would benefit the recovery of neuronal function after ICH.

Correspondence to: Dr Zongmao Zhao, Department of Neurosurgery, The Second Hospital of Hebei Medical University, 215 Heping Road, Shijiazhuang, Hebei 050000, P.R. China
E-mail: zzm692017@sina.com

Key words: intracerebral hemorrhage, calcium voltage-gated channel auxiliary subunit, thrombospondin, proteomics

Materials and methods

Animal model of ICH. A total of 28 adult male Sprague-Dawley rats (weight, 280-320 g; 7-10 weeks old), purchased from the Experimental Animal Science Center of Hebei Medical University (Shijiazhuang, China) were used in the present study. All animals were housed under the same conditions (atmospheric humidity, 50-60%; 25˚C; 12-h light/dark cycle) and were allowed free access to food and tap water. In the present study, the animal experiments complied with the regulations of the Animal Welfare Act of the National Institutes of Health Guide for the Care and Use of Laboratory Animals and were approved by the Ethics Committee of Hebei Medical University (IACUC Hebmu-Glp-2016017; Shijiazhuang, China).

The rats were randomly divided into seven groups as follows: The first was the sham group with injection of 10 μl saline into the striatum; the six other groups comprised rats that were injected with collagenase IV dissolved in 10 μl saline into the striatum and examined on days 1, 3, 5, 7, 14 or 21 post-injection. ICH was induced by the injection of collagenase IV into the globus pallidus. Collagenases are proteolytic enzymes that are present within cells in an inactive form. Collagenase is released in response to inflammation. Collagen is a substrate of collagenase and exists in the basal lamina of blood vessels in brain tissue. The infusion of collagenase into the brain damages blood vessels and the blood brain barrier to mimic ICH (24,25). The rats in the present study were anesthetized with 1% pentobarbital sodium (intraperitoneal; 30 mg/kg) and the rats were placed in a position such that their heads were fixed on a stereotactic frame (model SD252; NeuroStar) in order for the posterior and anterior fontanelle to be on the same horizontal plane. A hole at a diameter of 1 mm was drilled into the skull on the right side at 2.4 mm caudal to the bregma. The needle was inserted into the brain tissue at 6 mm deep. Collagenase IV (0.3 U in 1 μl; Sigma-Aldrich; Merck KGaA) was dissolved in 0.9% sterile saline and injected into the right globus pallidus with a Hamilton syringe at a speed of 0.2 μl/min (Fig. 1A and B). The sham control animals received an injection of 10 μl saline into the right globus pallidus. The hole in the skull was closed with bone wax and the wound was closed with a suture. The rats were placed in a warm box during the recovery period. For harvesting brain tissue samples, the rats were decapitated under anesthesia with intraperitoneal injection of 1% sodium pentobarbital at a dosage of 30 mg/kg. Brain samples were obtained on days 1, 3, 5, 7, 14 or 21 following the collagenase IV injection. Briefly, the rat brains were removed and the tissue surrounding the hematoma in the striatum was obtained under a light microscope to ensure the tissues were taken from the right location (Fig. 1C). Brain tissues were snap frozen in liquid nitrogen and then stored at -80˚C.

RNA extraction and reverse transcription-quantitative PCR (RT-qPCR). Following injection of saline (sham group) or collagenase IV, the rat brains were removed on days 1, 3, 5, 7, 14 or 21. The striatum on the side of the hematoma was used as the specimen, and the right striatum of rats (saline injection) was used as a control. Total RNA was extracted from the samples using TRIzol® reagent (Sangon Biotech Co., Ltd.) according to the manufacturer's instructions. Reverse transcription was performed according to the manufacturer's protocol using the RevertAid First Strand cDNA Synthesis Kit (Thermo Fisher Scientific, Inc.). The primers used for qPCR were designed and synthesized by Sangon Biotech Co., Ltd. Gel electrophoresis was used to screen the production of individual amplification products, standard curve analysis was used to screen the PCR efficiency and melting curve analysis was used to screen for the formation of primer-dimers. The sequences of the primers used were as follows: TSP1 forward, 5'-AAACTGTCCCTATGTGCC CAATGC-3' and reverse, 5'-TGCCGTCGTTGTCATCGT CATG-3' (92 bp); TSP2 forward, 5'-GCTTCCACTGCCTGC CTTGTC-3' and reverse, 5'-GCACGGATTCTCTGGCTC ACATAC-3' (110 bp); α2δ1 forward, 5'-CGTGGGTGGATA ACAGCAGAAC-3' and reverse, 5'-CAGAGTCAATCCGCT CACACTTCC-3' (144 bp); and β-actin forward, 5'-TGTCAC CAACTGGGACGATA-3' and reverse, 5'-GGGGTGTTG AAGGTCTCAAA-3'. β-actin (rat β-actin endogenous reference genes primers; product no. B661202-0001; purchased from Sangon Biotech Co., Ltd.) was used to normalize the total cDNA content and reverse transcription efficiency.

qPCR was performed using an ABI QuantStudio6Flex real-time fluorescence quantitative PCR instrument (Applied Biosystems; Thermo Fisher Scientific, Inc.) using SYBR-Green Chemical [SGExcel Fast SYBR Mixture (with ROX); Sangon Biotech Co., Ltd.]. All reactions were carried out under the following conditions: 20 μl reaction system (8.2 μl ddH_2O, 0.4 μl reverse primer, 0.4 μl forward primer, 1 μl template DNA and 10 μl mixture, which contained Fast Taq DNA Polymerase, PCR Buffer, dNTPs, SYBR Green, fluorescence dye, Mg^{2+} and ROX dye), with pre-denaturation at 95˚C for 3 min. This was followed by denaturation at 95˚C for 5 sec, annealing at 60˚C for 20 sec and extension at 60˚C for 20 sec for 40 cycles. The melting curve was analyzed at the temperature range of 60-95˚C. The melting curves of all samples were used as specific controls. All gene expression data were calculated using the $2^{-\Delta\Delta Cq}$ method, indicating an n-fold change in gene expression compared with the sham sample (26).

Western blot analysis. The striatum tissue on the hematoma side and the right striatum from rats in the sham group were added to RIPA lysis buffer (5X buffer; Beijing Solarbio Science & Technology Co., Ltd.) containing 1% inhibitor. Each mg of tissue was lysed with 10 μl lysate (1:10 ratio). Following ultrasonic homogenization, the lysate was centrifuged at 12,000 x g at 4˚C for 20 min. The supernatant was denatured with 5X buffer at 95˚C for 5 min, and the samples were aliquoted and stored at -80˚C. The protein concentration was determined using a BCA kit [PQ0011; Multisciences (Lianke) Biotech Co., Ltd.]. SDS-PAGE (6-12%) protein separation was performed using a rapid gel kit (ZD304A-1; Beijing Zoman Biotechnology Co., Ltd.) and protein was transferred to a PVDF membrane. Due to the low levels of TSP1 in the brain tissue and the high molecular weight, and in order to more effectively separate TSP1 protein and separate internal reference proteins simultaneously, the separation gel for gel electrophoresis was configured with a concentration of 6% in the upper layer and 8% in the lower layer. The sample amount loaded was 80 μg total

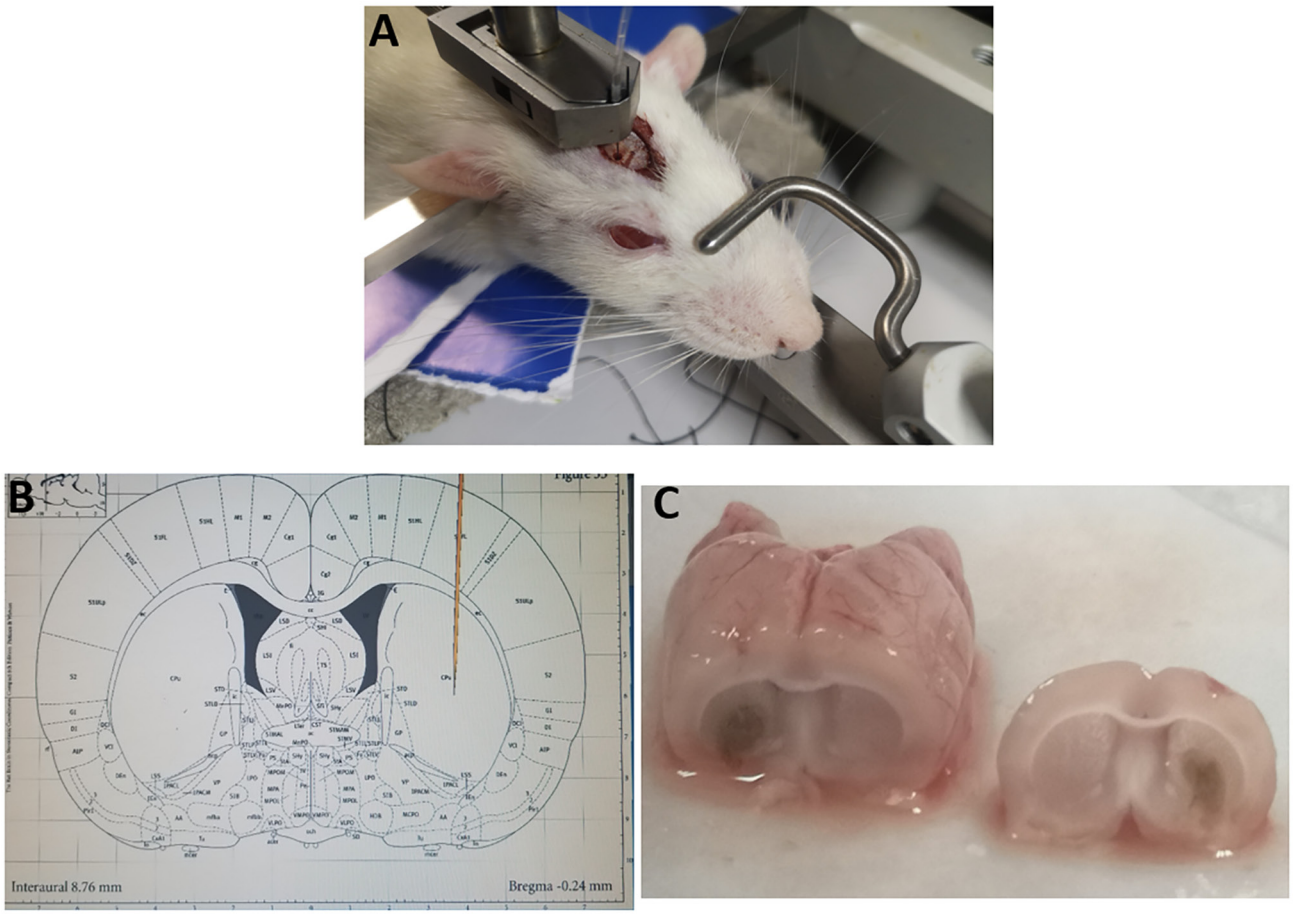

Figure 1. Establishment of a model of intracerebral hemorrhage. (A) Rats were fixed on the stereotactic frame. (B) Anatomical map of the brain of the stereotactic system indicating the location of the puncture. (C) Following the injection of collagenase IV into the brains of the rats, the rats were decapitated, and the brains were collected. A representative image of the brain at 72 h is shown. The shape and location of the hematoma is shown along the coronal section of the puncture path.

protein per lane, and after separation, this was transferred at 100 V to a film for 2 h, which was subsequently blocked using 5% skimmed milk for 1.5 h at 4˚C. Incubation with the primary antibodies was performed in the refrigerator at 4˚C overnight, and incubation with secondary antibodies was performed at room temperature for 2 h. An Odyssey infrared laser scanning imaging system was used for PVDF film imaging. The primary antibodies used were as follows: TSP1 (dilution, 1:100; cat. no. MA5-13398; Invitrogen; Thermo Fisher Scientific, Inc.), TSP2 (dilution, 1:1,000; cat. no. GTX64459; GeneTex, Inc.), α2δ1 (dilution, 1:1,000; cat. no. ab2864; Abcam) and β-actin (dilution, 1:500,000; cat. no. AC026; ABclonal Biotech Co., Ltd.). The secondary antibodies used were mouse and rabbit antibodies (dilution, 1:1,000; rabbit IgG (H&L) Antibody Dylight™ 800-conjugated, cat. no. 611-145-122 and mouse IgG (H&L) Antibody Dylight™ 800 Conjugated, cat. no. 610-145-002; Rockland Immunochemicals Inc.). The bands were visualized using an ECL Plus Detection Kit (Thermo Fisher Scientific, Inc.). The protein bands were detected and the density was semi-quantified using the Odyssey IR fluorescence scanning imaging system (LI-COR Biosciences) and further analyzed using Adobe Photoshop (version CC2020; Adobe Systems, Inc.). Then, these values were normalized to the protein bands in the sham group.

Transcriptome sequencing, proteome quantitative analysis and combined analysis of the two groups. At the beginning of the experiment, three adult male Sprague-Dawley rats of the same age and weight as those in the aforementioned experiments were selected, and brain tissue samples surrounding the hematoma were obtained after 24 h following the establishment of the model. The samples were sent to Shanghai Applied Protein Technology Co., Ltd. for transcriptional sequencing and protein quantification, and the two were analyzed jointly. This experiment mainly analyzed the proteomics of samples through the steps and methods of protein extraction and peptide enzymolysis, TMT labeling, high pH reversed-phase peptide classification, liquid chromatography-tandem mass spectrometry data collection (Thermo Scientific Acclaim PepMap100; 100 μm x 2 cm; nanoViper C18; with positive ionization mode; Thermo Fisher Scientific, Inc.) with nitrogen gas temperature at 300˚C, nebuliser pressure (psi) of 5-15 psi and a flow rate of 5.0 l/min, protein identification, and quantitative analysis and bioinformatics analysis. The samples were chromatographically separated and analyzed by mass spectrometry using a Q-Exactive mass spectrometer. The precursor ion scanning range was 300-1,800 m/z, the primary mass spectrometry resolution was 70,000 at 200 m/z, the automatic gain control target was 1e6, the maximum injection time was 50 msec, and the dynamic exclusion time was 60.0 sec.

The mass-to-charge ratios of peptides and peptide fragments were collected as follows: 20 fragments were collected after each full scan (MS2 scan), the MS2 Activation Type was HCD, the isolation window was 2 m/z, MS2 resolution rate 17,500 at 200 m/z (TMT 6-plex) or 35,000 at 200 m/z (TMT 10-plex), normalized collision energy was 30 eV, underfill was 0.1%.

Total RNA was extracted from the brain tissues using TRIzol® reagent according to the manufacturer's instructions (Sangon Biotech Co., Ltd.). RNA samples were detected based on the A260/A280 absorbance ratio with a Nanodrop ND-2000 system (Thermo Fisher Scientific, Inc.), and the RNA integrity number was determined using an Agilent Bioanalyzer 4150 system (the nucleotide length was 350bp and a RNA Nano 6000 Assay Kit was used, obtained from Agilent Technologies Inc.).

Only qualified samples were used for library construction. Paired-end libraries were prepared using a ABclonal mRNA-seq Lib Prep Kit (Product: RK20303; ABclonal Biotech Co., Ltd.) according to the manufacturer's instructions. The mRNA was purified from 1 μg total RNA using oligo(dT) magnetic beads followed by fragmentation using divalent cations at elevated temperatures in ABclonal First Strand Synthesis Reaction Buffer (ABclonal Biotech Co., Ltd.). Subsequently, first-strand cDNAs were synthesized with random hexamer primers and Reverse Transcriptase (RNase H) using mRNA fragments as templates, followed by second-strand cDNA synthesis using DNA polymerase I, RNAseH, buffer and deoxynucleoside triphosphates. The synthesized double-stranded cDNA fragments were then adapter-ligated for preparation of the paired-end library. Adapter-ligated cDNA was used for PCR amplification. PCR products were purified (AMPure XP system) and library quality was assessed on an Agilent Bioanalyzer 4150 system (Agilent Technologies, Inc.). Finally, sequencing was performed using an Illumina Novaseq 6000/MGISEQ-T7 instrument (Illumina, Inc.).

Raw data were first processed through in-house perl scripts by removing the adapter sequence and filtering out reads of low quality (number of lines with a string quality value ≤25 accounts for >60% of the entire reading) and for which the N (base information cannot be determined) ratio was >5% to obtain clean reads for subsequent analysis. Subsequently, clean reads were separately aligned to the reference genome with orientation mode using HISAT2 v2.1.0 software (http://daehwankimlab.github.io/hisat2/) to obtain mapped reads. The mapped reads were analyzed with Stringtie software (version v2.0.4; http://ccb.jhu.edu/software/stringtie/), and then the Gffcompare software (version v1; http://ccb.jhu.edu/software/stringtie/gffcompare.shtml) was used to compare the mapped reads with the reference genome GTF/GFF file to find the original unannotated transcription region and discover novel transcripts and novel genes of the species. FeatureCounts (release, 2.0.0; http://subread.sourceforge.net/) was used to count the read numbers mapped to each gene. Furthermore, the fragments per kilobase of transcript per million mapped reads of each gene was calculated based on the length of the gene and read count mapped to this gene. Differential expression analysis was performed using DESeq2 (Bioconductor 3.9; http://bioconductor.org/packages/release/bioc/html/DESeq2.html). Differentially expressed genes (DEGs) with an adjusted P<0.05 were considered to be significantly DEGs. Alternative splicing in the RNA sequencing data was analyzed by rMATS (release, 4.0.2, http://rnaseq-mats.sourceforge.net/index.html).

Protein-protein interaction analysis was used to determine if there was an interaction between gene products and proteins. Protein-protein interactions were predicted based on the Search Tool for the Retrieval of Interacting Genes/Proteins (STRING) database (version 11.0; https://www.string-db.org/). First, the quantitative information of the target protein set was normalized to the (-1,1) interval. Then, the Complexheatmap R package (Release 3.14, https://cran.r-roject.org/src/base/R-3/) simultaneously classified the two dimensions of sample and protein expression (distance algorithm, Euclidean; connection, average linkage), and a hierarchical clustering heatmap was generated (https://bioconductor.org/packages/release/bioc/html/ComplexHeatmap.html).

Statistical analysis. GraphPad Prism 8 (GraphPad Software, Inc.) was used for data analysis. All data are presented as the mean ± SEM. Each experiment was repeated at least 3 times. An unpaired t-test or one-way ANOVA with Dunnett's post hoc test was used for statistical analyses. P<0.05 was considered to indicate a statistically significant difference.

Results

Changes in α2δ1 protein and mRNA expression in the ICH model. To determine the changes in α2δ1 expression in brain tissue around the hematoma following hemorrhage, the mRNA and protein levels of α2δ1 were detected. The α2δ1 mRNA levels began to decrease to 59±5% on the 1st day after the establishment of the model. The α2δ1 mRNA levels were significantly decreased on days 3 (15±4%), 5 (16±3%), 7 (11±3%), 14 (29±7%) and 21 (32±2%) (Fig. 2A). Detection of α2δ1 protein levels using western blot analysis revealed no significant difference compared with the sham group on days 1 (99.2±0.4%) and 3 (102.5±6.0%); however, these levels significantly increased to 123.5±4.8% on day 5, 136.4±5.7% on day 7 and 125.4±4.5% on day 14, subsequently decreasing to 97.4±4.7% on day 21 (Fig. 2B and C). The baseline levels were not different from the levels on day 21.

Changes in TSP1/2 protein and mRNA expression in the ICH model. To determine the changes in TSP1/2 protein expression following hemorrhage, the levels in the striatum around the hemorrhage were detected using western blot analysis. TSP1 protein expression gradually increased following hemorrhage to 135±10.6% on day 1 and 131.5±8.8% on day 3, reaching peak levels on day 5 (181.0±6.5%), and then gradually decreased to sham levels (Fig. 3A and B). The expression levels of TSP2 decreased to 54.3±6.4% on day 5 and 50.6±7.4% on day 7 following ICH; however, its expression increased to 183.8±26.6% on day 14 (Fig. 3C and D). The expression levels on days 1, 3 and 21 did not significantly differ from the basal expression levels. However, the changes in the mRNA levels did not completely coincide with those observed at the protein level. TSP1 mRNA levels began to

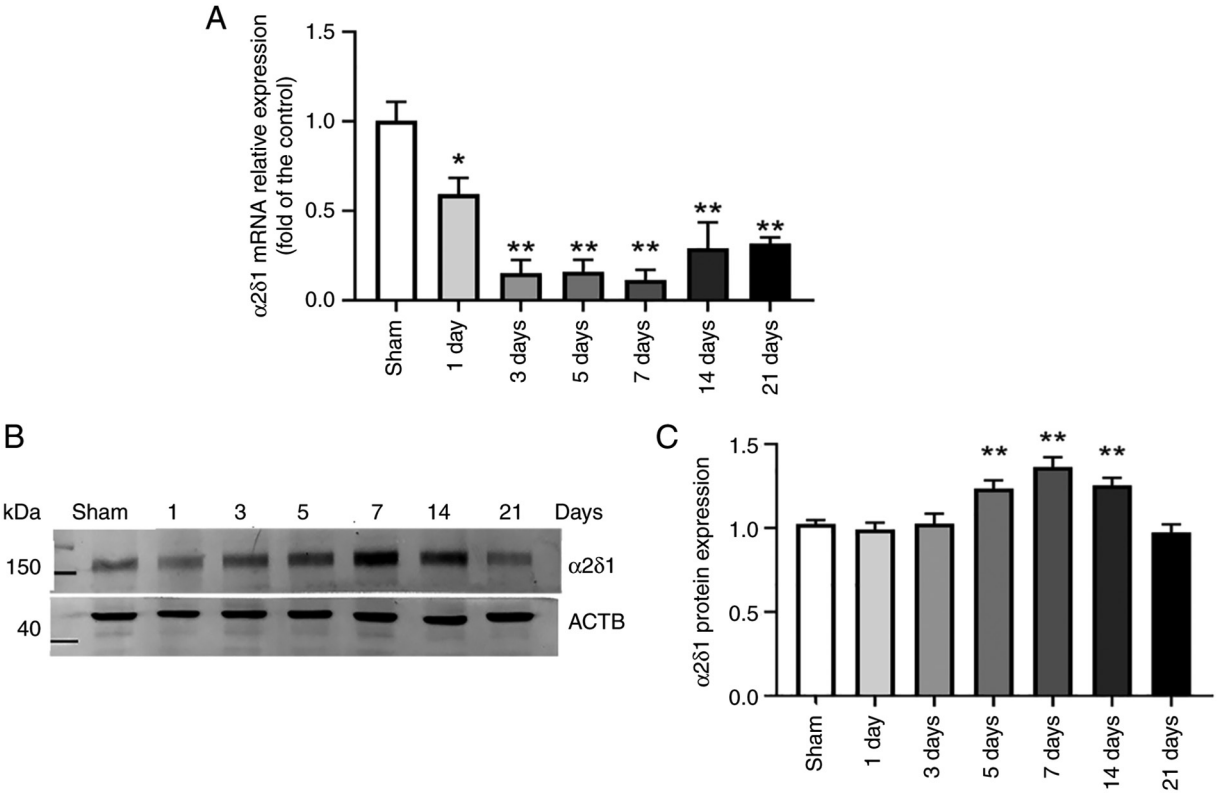

Figure 2. Changes in α2δ1 protein and mRNA expression following hemorrhage. (A) α2δ1 mRNA expression on days 1-21 after modeling was compared with that of the sham group. (B) Representative western blots of α2δ1 protein expression and (C) semi-quantification of the band density in the control group and at each time point in the modeling group. *P<0.05 and **P<0.0001 compared with the values in the sham group. α2δ1, calcium voltage-gated channel auxiliary subunit (Cacna2δ1); ACTB, β-actin.

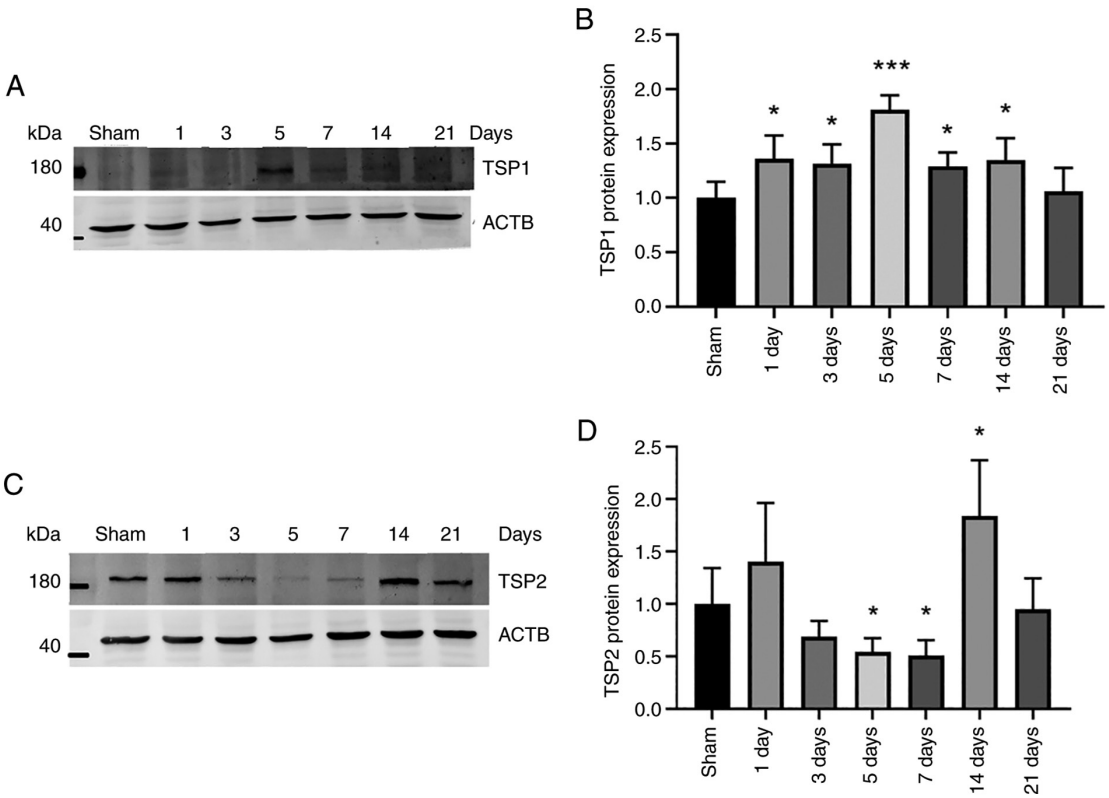

Figure 3. Changes in TSP1 and TSP2 protein expressoin following hemorrhage injury. (A) Representative western blots of TSP1 protein expression and (B) semi-quantification of the band density in the sham group and at each time point after modeling. (C) Representative western blots of TSP2 protein expression and (D) semi-quantification of the band density in the sham group and at each time point after modeling. *P<0.05 and ***P<0.0001 compared with the values in the sham group. ACTB, β-actin; TSP, thrombospondin.

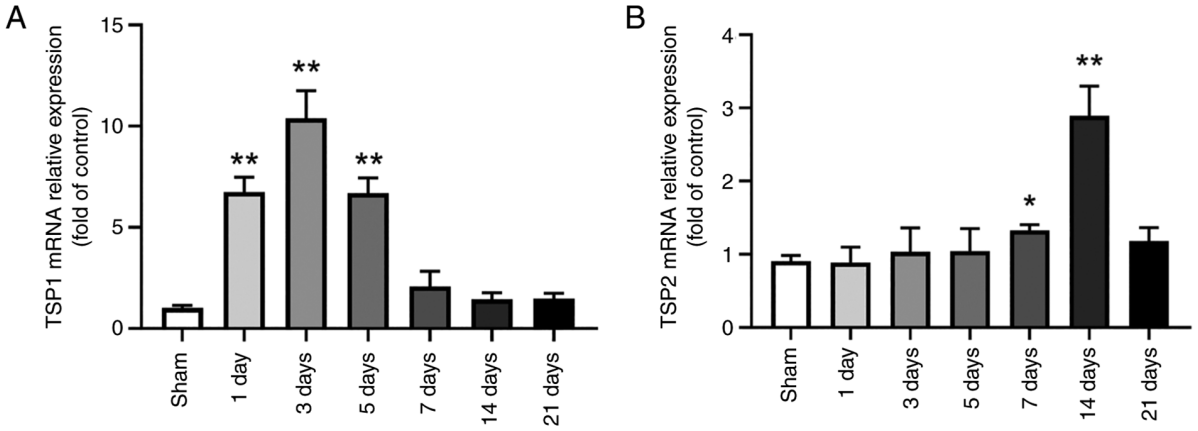

Figure 4. Changes in TSP1 and TSP2 mRNA expression following hemorrhage. mRNA expression levels of (A) TSP1 and (B) TSP2 were measured using reverse transcription-quantitative PCR at each time point after modeling and compared with those of the sham group. *P<0.05 and **P<0.01 compared with the values in the sham group. ACTB, β-actin; TSP, thrombospondin.

increase on the 1st day following ICH to 675±73%, reached peak levels of 1,039±136% on the 3rd day, and then began to recover to 670±74% on day 5, 208±74% on day 7, 144±33% on day 14 and 148±26% on day 21. No significant difference in expression was observed between the groups on the days 7, 14 and 21 and the sham group (P>0.05; Fig. 4A). Compared with the sham group, TSP2 mRNA expression did not increase or decrease significantly on days 1 (91±8%), 3 (103±33%) and 5 (105±31%) following ICH; however, its expression began to increase on day 7 to 133±8%, reaching peak levels on day 14 (289±41%), and decreasing to sham levels (118±18%) on day 21 (Fig. 4B). There was no significant difference compared with the sham group on day 21.

Analysis of DEGs related to TSP1 and α2δ1. To determine whether ICH alters gene and protein expression levels, DESeq2 was used to analyze the samples from ICH and sham animals with biological repetition. DEGs are displayed in the volcano plot and were analyzed using cluster analysis (Fig. 5A). It was revealed that 60 genes were increased >1.5-fold compared with those in sham tissues and 40 genes were decreased to <0.8-fold compared with those in sham tissues. The cluster map presents the top 60 upregulated genes and the top 40 downregulated genes (Fig. 5B). Proteins were also analyzed using proteomics analysis. It was revealed that 263 proteins exhibited a ≥1.2-fold increase and 52 proteins exhibited a ≤0.83-fold decrease compared with the control values. The quantitative results are shown in the volcano plot (Fig. 5C). The differentially expressed proteins in the ICH and control group were clustered and analyzed using the hierarchical cluster analysis and the data are displayed in the form of a heatmap (Fig. 5D).

By analyzing the 24-h striatal proteomics data, the regulatory association among the proteins in the STRING database was determined and some proteins were selected for mapping. The proteins with the largest difference were selected (Fig. 6). Based on the data shown in Fig. 2C, α2δ1 protein expression was significantly upregulated on days 5-14 and returned to baseline level on day 21. In addition, it was found that α2δ1 has a regulatory association with neural EGFL like 2 (Nell2), which has a regulatory association with TSP1, based on the STRING analysis.

Discussion

Both TSP1 and TSP2 are present in the developing brain and are proteins secreted by astrocytes (17). Their expression levels are low or non-existent in the adult rat brain (20). They have similar structures and the same functional domains (21). *In vitro* experiments have demonstrated that all subtypes of TSP can increase the number of synapses, and TSP1 and TSP2 have been reported to promote synaptic formation in the central nervous system (CNS) *in vivo* (20,21). Following the ischemic injury to the CNS, the levels of TSP1/2 are upregulated, while the lack of TSP1/2 impairs synaptic and functional recovery following ischemic stroke (4).

α2δ1 is highly expressed throughout the entire CNS (8) and is enriched in cortical and hippocampal neurons. As a receptor of TSP, α2δ1 is involved in the formation of excitatory synapses in the CNS (21). They interact through the synaptic EGF-like domain of TSP and the VWF-A domain of α2δ1, and the upregulation of α2δ1 in neurons enhances synaptic formation *in vivo* (21). α2δ1 serves an important role in the formation and maturation of excitatory synapses in the cerebral cortex (20). As an auxiliary subunit of voltage-gated calcium channels, a previous study (27) has focused on the regulation of calcium channel function and transport, including the interaction between gabapentin drugs and α2δ1. The role of α2δ1 in synaptic formation is not directly related to the expression levels or function of calcium channels (21). The expression levels of α2δ1 in the injured brain tissue increase following ischemia, which may be related to the activation of ion channels and the formation of synapses (12).

A previous study has reported the increase in TSP1/2 mRNA expression in the striatum following ICH (19). It is primarily hypothesized that TSP1/2 is related to the regulation of angiogenesis following hemorrhage, although not from the point of view of synaptic regeneration, and changes in TSP1/2 protein expression have not been reported with regard to synaptic regeneration (19). However, to the best of our knowledge, the expression levels of α2δ1 in brain tissues around the hematoma following ICH have not been reported to date. In the present study, a rat model of ICH was established by injection of collagenase IV. Through gene sequencing and

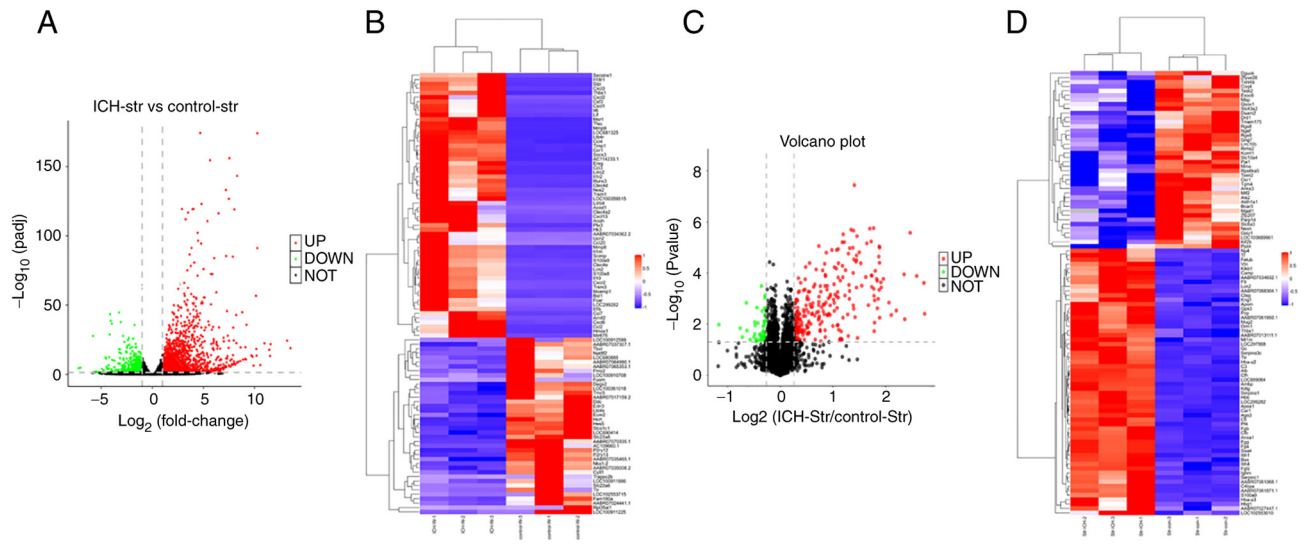

Figure 5. Analysis of differentially expressed genes and proteins. (A) Gene expression analysis for striatum tissues obtained from sham and ICH model animals indicating the changes in gene expression in the different samples. The scattered dots in the image represent genes, the black dots represent the genes with no significant difference, the red dots represent the upregulated genes with significant differences, and the green dots represent the downregulated genes with significant differences. (B) Differential gene cluster map (red indicates upregulation, blue indicates downregulation). (C) A volcano plot was drawn using the fold change of protein expression between the ICH and control samples. P-values were obtained using an unpaired t-test, indicating significant differences between the ICH and control samples. The abscissa is the multiple of difference (logarithmic transformation with base 2), the ordinate is the significant P-value (logarithmic transformation with base 10), the red dots represent proteins with a significant increase (fold change >1.2 and P<0.05), the green dots represent proteins with a significant decrease (fold change >0.8) and black dots represent proteins with no significant differences. (D) Hierarchical clustering analysis represented by a tree heatmap, in which each row represents one protein and columns represent one sample each (n=3 each for control and ICH samples). The protein expression with significant differences in the different samples is shown in the heatmap; red represents significantly upregulated proteins and blue represents significantly downregulated proteins. The gray area in the heatmap indicates no protein quantitative information. ICH, intracerebral hemorrhage; str, striatum.

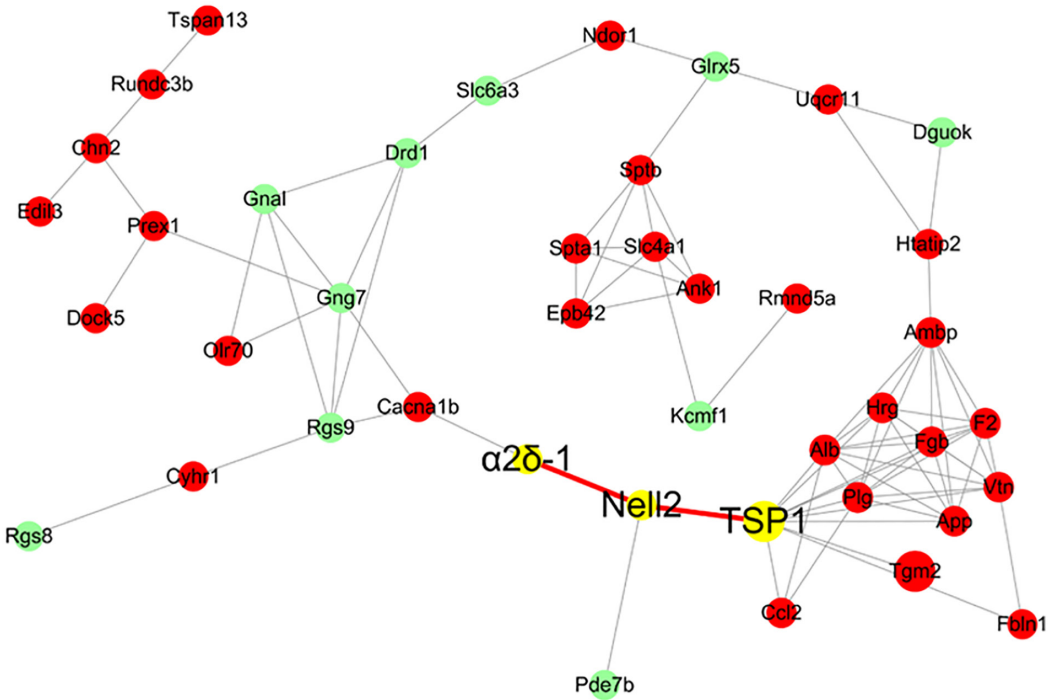

Figure 6. Protein-protein interaction network related to TSP1 and α2δ1. Red indicates upregulation and green indicates downregulation. The size of the dot indicates the degree to which it is connected to the surrounding area, the solid lines indicate that there is experimental evidence to support the regulatory association between two genes. The yellow dots and red solid lines highlight the position and association between TSP1 and α2δ1. TSP1, thrombospondin; α2δ1, calcium voltage-gated channel auxiliary subunit (Cacna2δ1).

quantitative protein analysis, it was revealed that the mRNA and protein expression levels of TSP1 in the striatum around the hematoma increased at 24 h after modeling; however, α2δ1 and TSP2 transcription was detected but not altered, whereas proteomics only detected α2δ1 but not TSP2. These data served a guiding role in setting the detection time of

the samples in the follow-up experiment. Furthermore, the results of western blot analysis and RT-qPCR revealed that the changes in TSP1 expression were consistent with the results of proteomics and transcriptome analyses, which increased the reliability of the experimental results. By performing western blot analysis of the brain tissue around the hematoma following ICH, it was revealed that the protein expression levels of α2δ1 increased following ICH, and the protein expression levels of TSP2 decreased and then increased, while TSP1 expression increased and then decreased. Peak TSP1 protein expression was observed after 5 days, peak TSP2 protein expression was observed after 14 days, and peak α2δ1 protein expression was observed after 7 days, which was between the peaks of TSP1 and TSP2.

Following ICH, the brain tissue is destroyed by the hematoma, and the number of synapses decreases (2). The increase in the α2δ1 and TSP1/2 expression may trigger synaptic regeneration, such as the recovery of the number and structure of synapses (4,20,21). Therefore, synaptic regeneration following ICH is an important recovery process for neuronal function. However, no approaches are currently available that can increase the expression of these proteins following cerebral hemorrhage in order to promote the healing process and recovery of patients. The findings of the present study may provide useful information for the development of novel approaches that may be used to increase α2δ1 and TSP1/2 expression in damaged brain tissues following ICH. However, each protein in the body may serve multiple roles and participate in a variety of mechanisms. The increase in the levels of α2δ1 and TSP1/2 may not necessarily be caused by synaptic regeneration.

Both α2δ1 and TSP1 interacted with Nell2. It is possible that Nell2 is also involved in the regeneration and reconstruction of nerve synapses. α2δ1 mRNA expression decreased following ICH, which was not consistent with that of its protein expression levels. At present, a satisfactory explanation cannot be provided for this phenomenon. Therefore, further studies are warranted. ICH may alter gene transcription and translation, affecting the expression of α2δ1 and other proteins. TSP1 and TSP2 are proteins secreted by glial cells that are involved in synaptic production in the CNS (19). In addition, the mechanisms of synaptogenesis and regulation of synaptogenesis and degeneration are complex. Each type of astrocyte may exhibit different synaptic and anti-synaptic factors. It has been demonstrated that a variety of substances secreted by glial cells, such as secreted protein acidic and rich in cysteine, Hevin, and glypicans 4 and 6, are involved in this process, as well as in the mechanisms of the α2δ1 interaction with TSP1/2 to promote synaptogenesis (28). The synaptic potential in each brain region may differ and may be heterogeneous, which is mainly due to differences in the gene expression profiles, leading to the secretion of various concentrations of synaptic proteins with different synaptogenic potential (29). However, there is a phenomenon of the regional restricted distribution of astrocytes in the CNS, and there is no evidence of a second tangential migration, even after acute injury to the CNS, which reveals the inherent limitations of the response of astrocytes to injury (30). In the CNS, synapses can be wrapped by astroglial processes, which are often termed peri-synaptic astroglial processes (31). The close association between peri-synaptic astrocytic processes (31) and neurons provides an indispensable factor for the formation of neural circuits, and may provide a relatively airtight environment for synaptic formation and regulation. This demonstrates the complexity of synaptogenesis and regulation in the CNS. The present study only revealed the changes in α2δ1 and TSP1/2 expression in the tissue around the hematoma following ICH. However, the possibility that the increased expression of these proteins in the brain produces other unexpected effects cannot be ruled out. For example, TSP1/2 proteins are involved in regulating blood vessel regeneration following ICH (19). However, it is not yet clear whether the upregulation of α2δ1 increases intracellular Ca^{2+} levels to exert an unexpected effect on neuron recovery. The expression levels of α2δ1 and TSP1/2 in other areas of the CNS and whether these serve a dominant role in the regulation of synapses in different brain regions remains unclear; thus, the regulatory mechanisms of synaptic recovery following nerve injury warrant further investigation.

The findings of the present study suggested that the expression levels of α2δ1 and TSP1/2 were increased in brain tissues in response to ICH. These alterations may serve an important role in the recovery of neurons and synapses in response to the ischemia and hypoxia during ICH. The changes in the molecular and cellular levels are the foundation of the neurological functional recovery.

Acknowledgements

Not applicable.

Funding

The present study was supported by National Key R&D Program Intergovernmental Cooperation on International Scientific and Technological Innovation of the Ministry of Science and Technology of China (grant no. 2017YFE0110400); National Natural Science Foundation of China (grant no. 81870984); Hebei Natural Science Foundation General Project-Beijing-Tianjin-Hebei Basic Research Cooperation Project (grant no. H2018206675); Special Project for the Construction of Hebei Province International Science and Technology Cooperation Base (grant no. 193977143D); Government-funded Project on Training of Outstanding Clinical Medical Personnel and Basic Research Projects of Hebei Province in the Year of 2017; and Government-funded Project on Training of outstanding Clinical Medical Personnel and Basic Research Projects of Hebei Province in the Year of 2019.

Availability of data and materials

The datasets generated and/or analyzed during the current study are available in the SRA database repository (https://www.ncbi.nlm.nih.gov/sra/?term=PRJNA797360). The other datasets used and/or analyzed during the current study are available from the corresponding author on reasonable request.

Authors' contributions

BW, XL, NY, CN, LG and ZZ conceived and designed the study. BW, XL, NY, LY, CN and LG collected data. BW, XL,

NY, LY and ZZ analyzed and interpreted the data. BW, XL, NY, LY, CN and LG collected materials and samples. BW, XL, NY, CN, LG and ZZ drafted the manuscript. BW and ZZ confirm the authenticity of all the raw data. All the authors have read and approved the final manuscript.

Ethics approval and consent to participate

The animal experiments complied with the regulations of the Animal Welfare Act of the National Institutes of Health Guide for the Care and Use of Laboratory Animals (NIH Publication no. 85-23, revised in 1996) and were approved by the Ethics Committee of Hebei Medical University (IACUC Hebmu-Glp-2016017, Shijiazhuang, China).

Patient consent for publication

Not applicable.

Competing interests

The authors declare that they have no competing interests.

References

1. Qureshi AI, Mendelow AD and Hanley DF: Intracerebral haemorrhage. Lancet 373: 1632-1644, 2009.
2. Dancause N, Barbay S, Frost SB, Plautz EJ, Chen D, Zoubina EV, Stowe AM and Nudo RJ: Extensive cortical rewiring after brain injury. J Neurosci 25: 10167-10179, 2005.
3. Ito U, Kuroiwa T, Nagasao J, Kawakami E and Oyanagi K: Temporal profiles of axon terminals, synapses and spines in the ischemic penumbra of the cerebral cortex: Ultrastructure of neuronal remodeling. Stroke 37: 2134-2139, 2006.
4. Liauw J, Hoang S, Choi M, Eroglu C, Choi M, Sun GH, Percy M, Wildman-Tobriner B, Bliss T, Guzman RG, *et al*: Thrombospondins 1 and 2 are necessary for synaptic plasticity and functional recovery after stroke. J Cereb Blood Flow Metab 28: 1722-1732, 2008.
5. Keep RF, Hua Y and Xi G: Intracerebral haemorrhage: Mechanisms of injury and therapeutic targets. Lancet Neurol 11: 720-731, 2012.
6. Veltkamp R and Purrucker J: Management of spontaneous intracerebral hemorrhage. Curr Neurol Neurosci Rep 17: 80, 2017.
7. Risher WC and Eroglu C: Thrombospondins as key regulators of synaptogenesis in the central nervous system. Matrix Biol 31: 170-177, 2012.
8. Arikkath J and Campbell KP: Auxiliary subunits: Essential components of the voltage-gated calcium channel complex. Curr Opin Neurobiol 13: 298-307, 2003.
9. Cole RL, Lechner SM, Williams ME, Prodanovich P, Bleicher L, Varney MA and Gu G: Differential distribution of voltage-gated calcium channel alpha-2 delta (alpha2delta) subunit mRNA-containing cells in the rat central nervous system and the dorsal root ganglia. J Comp Neurol 491: 246-269, 2005.
10. Taylor CP and Garrido R: Immunostaining of rat brain, spinal cord, sensory neurons and skeletal muscle for calcium channel alpha2-delta (alpha2-delta) type 1 protein. Neuroscience 155: 510-521, 2008.
11. Zhang GF, Chen SR, Jin D, Huang Y, Chen H and Pan HL: α2δ-1 Upregulation in primary sensory neurons promotes NMDA receptor-mediated glutamatergic input in resiniferatoxin-induced neuropathy. J Neurosci 41: 5963-5978, 2021.
12. Luo Y, Ma H, Zhou JJ, Li L, Chen SR, Zhang J, Chen L and Pan HL: Focal cerebral ischemia and reperfusion induce brain injury through α2δ-1-bound NMDA receptors. Stroke 49: 2464-2472, 2018.
13. Li J, Song G, Jin Q, Liu L, Yang L, Wang Y, Zhang X and Zhao Z: The α2δ-1/NMDA receptor complex is involved in brain injury after intracerebral hemorrhage in mice. Ann Clin Transl Neurol 8: 1366-1375, 2021.
14. Bornstein P: Matricellular proteins: An overview. Matrix Biol 19: 555-556, 2000.
15. Lawler J: The structural and functional properties of thrombospondin. Blood 67: 1197-1209, 1986.
16. Adams J and Lawler J: Extracellular matrix: The thrombospondin family. Curr Biol 3: 188-190, 1993.
17. Adams JC: Thrombospondins: Multifunctional regulators of cell interactions. Annu Rev Cell Dev Biol 17: 25-51, 2001.
18. Lawler J: Thrombospondin-1 as an endogenous inhibitor of angiogenesis and tumor growth. J Cell Mol Med 6: 1-12, 2002.
19. Zhou HJ, Zhang HN, Tang T, Zhong JH, Qi Y, Luo JK, Lin Y, Yang QD and Li XQ: Alteration of thrombospondin-1 and -2 in rat brains following experimental intracerebral hemorrhage. Laboratory investigation. J Neurosurg 113: 820-825, 2010.
20. Christopherson KS, Ullian EM, Stokes CC, Mullowney CE, Hell JW, Agah A, Lawler J, Mosher DF, Bornstein P and Barres BA: Thrombospondins are astrocyte-secreted proteins that promote CNS synaptogenesis. Cell 120: 421-433, 2005.
21. Eroglu C, Allen NJ, Susman MW, O'Rourke NA, Park CY, Ozkan E, Chakraborty C, Mulinyawe SB, Annis DS, Huberman AD, *et al*: Gabapentin receptor alpha2delta-1 is a neuronal thrombospondin receptor responsible for excitatory CNS synaptogenesis. Cell 139: 380-392, 2009.
22. Yabkowitz R, Mansfield PJ, Ryan US and Suchard SJ: Thrombospondin mediates migration and potentiates platelet-derived growth factor-dependent migration of calf pulmonary artery smooth muscle cells. J Cell Physiol 157: 24-32, 1993.
23. Lin TN, Kim GM, Chen JJ, Cheung WM, He YY and Hsu CY: Differential regulation of thrombospondin-1 and thrombospondin-2 after focal cerebral ischemia/reperfusion. Stroke 34: 177-186, 2003.
24. Andaluz N, Zuccarello M and Wagner KR: Experimental animal models of intracerebral hemorrhage. Neurosurg Clin N Am 13: 385-393, 2002.
25. Rosenberg GA, Mun-Bryce S, Wesley M and Kornfeld M: Collagenase-induced intracerebral hemorrhage in rats. Stroke 21: 801-807, 1990.
26. Livak KJ and Schmittgen TD: Analysis of relative gene expression data using real-time quantitative PCR and the 2(-Delta Delta C(T)) method. Methods 25: 402-408, 2001.
27. Davies A, Hendrich J, Van Minh AT, Wratten J, Douglas L and Dolphin AC: Functional biology of the alpha(2)delta subunits of voltage-gated calcium channels. Trends Pharmacol Sci 28: 220-228, 2007.
28. Risher WC, Kim N, Koh S, Choi JE, Mitev P, Spence EF, Pilaz LJ, Wang D, Feng G, Silver DL, *et al*: Thrombospondin receptor α2δ-1 promotes synaptogenesis and spinogenesis via postsynaptic Rac1. J Cell Biol 217: 3747-3765, 2018.
29. Buosi AS, Matias I, Araujo APB, Batista C and Gomes FCA: Heterogeneity in synaptogenic profile of astrocytes from different brain regions. Mol Neurobiol 55: 751-762, 2018.
30. Tsai HH, Li H, Fuentealba LC, Molofsky AV, Taveira-Marques R, Zhuang H, Tenney A, Murnen AT, Fancy SP, Merkle F, *et al*: Regional astrocyte allocation regulates CNS synaptogenesis and repair. Science 337: 358-362, 2012.
31. Heller JP and Rusakov DA: Morphological plasticity of astroglia: Understanding synaptic microenvironment. Glia 63: 2133-2151, 2015.